Tehran University of Medical Sciences Publication
http://tums.ac.ir

Iran J Parasitol

Open access Journal at
http://ijpa.tums.ac.ir

Iranian Society of Parasitology
http://isp.tums.ac.ir

Original Article

Green Synthesized Gold Nanoparticles Ameliorate the *Toxoplasma gondii* Infection in Immunosuppressed Mice

Leila Masoori [1], Ruaa Majid Khazaal [2], Marzieh Rashidipour [1], Maryam Sepahvand [3], *Hossein Mahmoudvand [4]

1. *Razi Herbal Medicines Research Center, Lorestan University of Medical Sciences, Khorramabad, Iran*
2. *Department of Medical Laboratory Techniques, Nasiriyah Technical Institute, Southern Technical University, Nasiriyah, Iraq*
3. *Student Research Committee, Lorestan University of Medical Sciences, Khorramabad, Iran*
4. *Hepatitis Research Center, Lorestan University of Medical Sciences, Khorramabad, Iran*

Received 21 Feb 2026
Accepted 14 May 2026

Keywords:
Toxoplasmosis;
Immunosuppression;
Nanomedicine;
Bradyzoites

***Correspondence Email:**
dmahmodvand@gmail.com

Abstract

Background: In immunocompromised individuals, *Toxoplasma gondii* infection can disseminate rapidly, causing severe cerebral and visceral complications. This study aimed to synthesize gold nanoparticles (AuNPs) via green synthesis and evaluate their therapeutic efficacy and mechanisms in immunosuppressed murine models of toxoplasmosis.

Methods: Mice were immunosuppressed using dexamethasone prior to infection with the Tehran strain of *T. gondii*. AuNPs were administered orally at 0.5 and 1 mg/kg, alone or combined with pyrimethamine (PYR; 10 mg/kg), in a 0.2 mL volume for 14 days. Survival rates were monitored daily. Brain cyst number and size were assessed microscopically. Oxidative stress markers, cytokine levels, and bradyzoite surface antigen 1 (BAG1) gene expression were analyzed by real-time PCR.

Results: Synthesized AuNPs exhibited cubic morphology with an average size of 20–30 nm. Combined AuNPs–PYR treatment significantly improved survival and reduced brain cyst burden (P=0.001). Treatment markedly decreased malondialdehyde (MDA) levels while enhancing glutathione peroxidase (GPx) and superoxide dismutase (SOD) activity (P<0.01). Gene expression analysis demonstrated downregulation of BAG1 and IL-4 (<1.3-fold) alongside upregulation of IFN-γ and IL-12 (>4-fold). Hepatic and renal biomarkers were also significantly improved.

Conclusion: AuNPs, particularly in combination with PYR, demonstrate significant efficacy against toxoplasmosis in immunosuppressed murine models. Clinical trials are warranted to further assess the safety and therapeutic potential of this combination approach.

Introduction

Toxoplasmosis is an infectious disease caused by the obligate intracellular protozoan parasite *Toxoplasma gondii*, which can infect a diverse array of hosts, including humans (1). In immunocompetent individuals, primary infection with *T. gondii* is frequently asymptomatic or presents with nonspecific clinical features, such as mild lymphadenopathy. Nonetheless, in uncommon instances, the infection may result in significant organ involvement (2). In individuals with compromised immune systems, including those with HIV, organ transplant recipients, or patients undergoing immunosuppressive therapy, primary infection with *T. gondii* poses a significant health risk. The parasite can disseminate rapidly throughout the body, leading to severe infections affecting the brain, eyes, and lungs. Unlike immunocompetent individuals, these patients are unable to effectively control the acute phase of the infection, which may result in life-threatening complications (3, 4).

The conventional treatment protocol generally comprises a combination of pyrimethamine and sulfadiazine, supplemented with folinic acid to reduce the risk of bone marrow toxicity. When first-line medications are contraindicated or not well tolerated, alternative therapeutic agents such as spiramycin (notably during pregnancy), clindamycin, or minocycline may be employed (5). However, these pharmacological interventions are often linked to adverse effects, including myelosuppression, hypersensitivity reactions, gastrointestinal intolerance, and teratogenic risks, especially during the first trimester of pregnancy (5). Furthermore, specific strains of *T. gondii* have exhibited significant resistance to widely utilized pharmacological inhibitors in experimental models (6). Despite considerable progress in the development of antiparasitic agents and enhancements in their safety profiles, a definitive, safe, and universally efficacious therapeutic approach addressing both the acute and chronic phases of toxoplasmosis remains an unresolved clinical challenge.

Nanoparticles (NP) are defined as substances with dimensions not exceeding one hundred nanometers, which is a distinctive characteristic of these materials (7). Among metal nanoparticles, gold nanoparticles (AuNP) are recognized for their low toxicity, high stability, and catalytic properties, which confer a range of biological functionalities in medical applications, including antibacterial, antiviral, antifungal, and antimalarial activities (8). The application of herbal extracts in nanoparticle synthesis, commonly referred to as "green synthesis," simplifies the process and accelerates its progression (9, 10). The utilization of plant extracts for the synthesis of metal nanoparticles, particularly gold, has shown considerable potential, with various plants such as cinnamon, licorice, black tea, and eucalyptus being employed in the production of gold nanoparticles to date (10). In recent years, numerous studies have explored the *in vitro* and in vivo anti-*Toxoplasma* properties of various metal nanoparticles such as silver, copper, zinc, gold, platinum, and tellurium nanoparticles. However, the findings have been inconsistent and, at times, contradictory due to the effectiveness of the nanoparticles, potentially due to a range of factors, including the methods of synthesis, the specific strains of the parasite, and the techniques employed for application (11, 12). *Satureja khuzistanica* Jamzad, an endemic species of the Lamiaceae family native to Iran, is characterized by a high concentration of carvacrol and demonstrates significant antimicrobial, antioxidant, anti-inflammatory, and analgesic activities. Research indicates its potential therapeutic applications in the management of infectious and metabolic diseases, as well as its protective effects against oxidative damage in critical organs including the liver and kidneys (13).

Considering the biological and pharmacological properties of AuNP and this plant, the present study focused on the green synthesis of AuNP and conducted a comprehensive investigation into the therapeutic effects and potential mechanisms of action of these nanoparticles in combating *T. gondii* infection in immunocompromised murine models.

Materials and Methods

AuNP green synthesis

Aerial parts of *Satureja khuzestanica* were procured in 2024 from Kimia Daru Aflak Company, Khorramabad, Iran. The dried plant material was powdered and dissolved in distilled water at a 10:1 ratio. The mixture was agitated on a shaker at 180 rpm for 60 min to facilitate the release of bioactive compounds, followed by ultrasonic treatment at 60 °C for 40 min to enhance extraction efficiency. The extract was then concentrated under vacuum at 40 °C using a rotary evaporator and stored in opaque containers at ambient temperature until further use. For the biosynthesis of gold nanoparticles, the plant extract was reacted with a gold tetrachloride ($HAuCl_4$) solution (Sigma-Aldrich, Taufkirchen, Germany). Successful nanoparticle formation was indicated by a color change of the solution from light yellow to dark red (14, 15).

Physicochemical Characterization of AuNPs

UV-vis spectroscopy was performed on a 1:10 diluted sample within the 350–680 nm wavelength range (LSI-Alpha spectrophotometer) to monitor synthesis progress. Morphological characterization was conducted by scanning electron microscopy (SEM; Hitachi S-4160, 15 kV, 1 nm resolution). XRD crystallography was carried out over a 10–80° scanning range using Cu Kα radiation (λ = 1.52 Å; GNR Explorer, Italy). FTIR spectroscopy was performed on AuNPs mixed with KBr (25:250 mg ratio) across 400–4000 cm^{-1} (Agilent Cary 630, Germany) to identify functional groups involved in nanoparticle synthesis and stabilization.

Animals and ethics

A total of 64 male BALB/c mice (25–30 g, 4–6 weeks old) were housed under controlled conditions with ad libitum access to food and water, in accordance with established guidelines for the Care and Use of Laboratory Animals. This study was approved by the Ethics Committee of Lorestan University of Medical Sciences, Iran (IR.LUMS.REC.1404.229).

Induction of Immunodeficiency in the Animal Model

To induce immunosuppression in mice, dexamethasone (Sigma-Aldrich, Germany) was administered orally at a dosage of 0.25 mg/kg body weight daily for 14 consecutive days prior to the inoculation with *Toxoplasma* cysts. This regimen was maintained throughout the experimental period without modification (16).

Induction of Infection and Establishment of Chronic Toxoplasmosis

The chronic toxoplasmosis model was established using the Tehran strain of *T. gondii*. Each mouse received an intraperitoneal injection of 0.5 ml of a brain homogenate suspension derived from an infected donor mouse, containing 20 to 25 cysts, supplemented with penicillin and streptomycin antibiotics (17).

Study design and grouping

Mice were randomly allocated into eight groups (N=8 each): healthy controls (NINI); *T. gondii*-infected, non-immunosuppressed (TINI); and six immunosuppressed-infected groups receiving normal saline (TIINS), PYR 20 mg/kg (TIIP20), AuNP 0.5 mg/kg (TIIA0.5), AuNP 1 mg/kg (TIIA1), AuNP 0.5 mg/kg + PYR 10 mg/kg (TIIP10+A0.5), or AuNP 1 mg/kg + PYR 10 mg/kg (TIIP10+A1). Oral treatment (0.2 mL) commenced two weeks post-inoculation with *T. gondii* cysts and continued for 14 days. AuNP

doses were selected based on pilot toxicity studies, and mortality was recorded daily throughout the experimental period (18).

Sample collection

Following a treatment duration of 14 d, which corresponds to 8 wk post-inoculation with the *Toxoplasma* parasite, all mice were subjected to deep anesthesia using a combination of ketamine and xylazine at the ratio 100:10 mg/kg (18). The whole brain tissue as well as blood specimens gathered from mice heart were collected and kept for further experiments.

Evaluating the parasite load and size of tissue cysts in brain

After preparing smears provided from brain tissue, the number and size of *T. gondii* tissue cysts were microscopically checked and recorded (19).

Evaluation of the tissue level of oxidant/antioxidant factors

Brain tissue homogenates were prepared, and the levels of malondialdehyde (MDA), superoxide dismutase (SOD), and glutathione peroxidase (GPx) in the samples were quantified using commercially available assay kits from Karmania Pars Gene and Kiazist (Iran), following the manufacturers' instructions.

Evaluating the gene expression level by Real-time PCR

Total RNA was extracted from brain tissue using a commercial kit (Parstous, Iran) per manufacturer's instructions, followed by DNase I treatment (Qiagen, Germany) to eliminate DNA contamination. RNA integrity was confirmed by 1.5% agarose gel electrophoresis, and cDNA synthesis was performed using a Sinaclon kit (Iran). Gene-specific primers for BAG1, IFN-γ, IL-12, and IL-4 (Table 1) were verified via NCBI database, and primer specificity was confirmed using BLAST Gene. qRT-PCR was conducted in a 20 µL reaction containing SYBR Green master mix (Pishgam, Iran), 1 µL each of forward and reverse primers (10 pM), 1 µL cDNA, and 7 µL sterile water. Thermal cycling conditions comprised initial denaturation at 94°C for 8 min, followed by 40 cycles of 95°C for 13 sec and 57°C for 35 sec. Relative expression was calculated using the $2^{-}\Delta\Delta CT$ method with β-actin as the reference gene, analyzed on a Bio-Rad iQ5 system (18, 19).

Table 1: Primer sequences employed for quantitative real-time polymerase chain reaction (qPCR) analysis

Primer	Sequence (5'–3')
BAG1	F: AGTCGACAACGGAGCCATCGTTATC R: ACCTTGATCGTGACACGTAGAACGC
IFN-γ	F: ATGAACGCTACACACTGCATC R: CCATCCTTTTGCCAGTTCCTC
IL-12	F: ACGACATTCGTCAACTGCAA R: TAAATTGGCACCCTGTAGGC
Il-4	F: ATCATCGGCATTTTGAACGAGGTC R: ACCTTGGAAGCCCTACAGACGA
β-actin	F: GTGACGTTGACATCCGTAAAGA R: GCCGGACTCATCGTACTCC

Biochemical analysis

The collected blood samples underwent centrifugation using a MiniSpin centrifuge (Eppendorf, Germany). The resulting sera were subsequently utilized to assess liver enzymes, specifically alanine transaminase (ALT) and aspartate transaminase (AST), as well as renal parameters, including blood urea nitrogen (BUN) and creatinine (Cr). These measurements were conducted employing the radi-

oimmunoassay technique with Pars Azmon kits (Tehran, Iran) and an autoanalyzer (RA 1000, Technicon Instruments, USA) (20).

Statistical analysis

Analysis of variance (ANOVA), complemented by Tukey's test and additional post-hoc analyses, was employed to perform a comprehensive evaluation of the data using SPSS software ver. 24.0 (IBM Corp., Armonk, NY, USA). Statistical significance was determined at a threshold of $P<0.05$.

Results

Physicochemical analysis of AuNP

The synthesized AuNP demonstrated uniform distribution and homogeneity (Supplementary File 1). Rapid reduction of gold ions by *S. khuzestanica* extract promoted homogeneous nucleation, yielding cubic-morphology nanoparticles (20–30 nm) stabilized by extract-derived biomolecules acting as capping agents. UV-Vis spectroscopy confirmed AuNP formation via an absorption peak at 511 nm. XRD diffraction peaks at 2θ = 38.15°, 44.33°, and 77.62° corresponded to the (111), (200), (220), and (311) Bragg planes of the face-centered cubic gold structure, consistent with JCPDS file 80-3697. FTIR spectra of the extract and AuNPs exhibited comparable profiles, confirming successful green synthesis. Identified infrared bands indicated multiple functional groups, including C–O (1078 cm^{-1}), C–O–C (1268 cm^{-1}, indicative of oligosaccharides or triacylglycerols), O–H (3412 cm^{-1}), and C–H (2936 cm^{-1}, associated with carbohydrates). Peaks within the 1618–2029 cm^{-1} range were attributed to Csp^3–H, C=C, and C=O stretching vibrations.

Parasitological assessment

After 14 days of treatment, survival rates were 100% in the TINI, TIIP20, TIIP10+A0.5, and TIIP10+A1 groups, compared to 87.5%, 75%, and 62.5% in the TIIA1, TIIA0.5, and TIINS groups, respectively ($P<0.05$). The greatest reductions in brain cyst number were observed in the TIIP10+A1 (no cysts, $P=0.000$) and TIIP10+A0.5 (0.625 cysts, $P=0.000$) groups, followed by TIIP20 (43.5 cysts, $P=0.009$), TIIA1 (76.6 cysts, $P=0.017$), and TIIA0.5 (106.3 cysts, $P=0.027$), relative to TIINS (672.4 cysts). Similarly, cyst size was most markedly reduced in TIIP10+A1 (no cysts, $P=0.000$) and TIIP10+A0.5 (10.2 nm, $P<0.001$), followed by TIIP20 (41.1 nm, $P=0.000$), TIIA1 (59.3 nm, $P<0.01$), and TIIA0.5 (72.6 nm, $P<0.01$), compared to TIINS (108.2 nm) (Fig. 1).

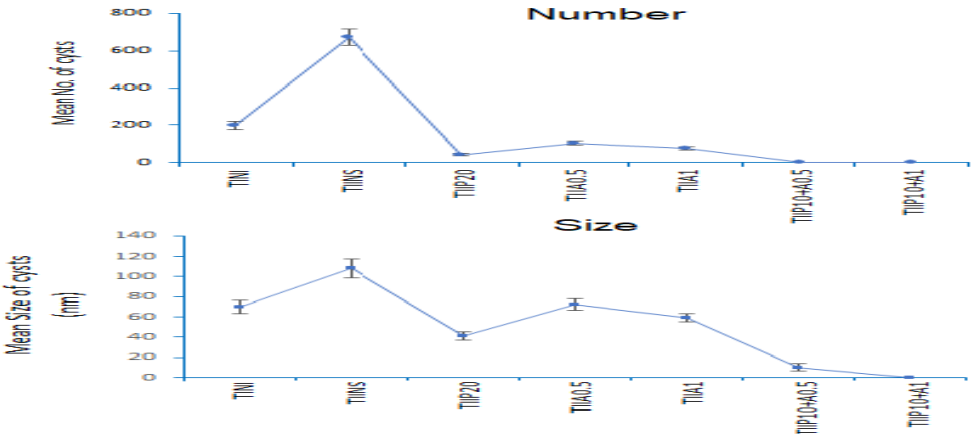

Fig. 1: Effects of AuNPs and PYR on the number and size of *T. gondii* tissue cysts in dexamethasone-immunosuppressed mice, as assessed by microscopic analysis. Data are expressed as mean ± SD (N=8)

Effect on oxidant/antioxidant markers

Infection with *T. gondii* mainly in immunosuppressed mice led to a marked elevation in the oxidative stress biomarker MDA and a concomitant reduction in the tissue levels of the antioxidant enzymes SOD and GPx (P=0.000). Conversely, ANOVA and post hoc analysis revealed that the administration of AuNP, particularly in the TIIP10+A0.5 (P=0.000) and TIIP10+A1 (P=0.000) groups, led to a significant reduction in MDA concentrations, as well as a marked increase (P=0.000) in the levels of GPx and SOD (Fig. 2).

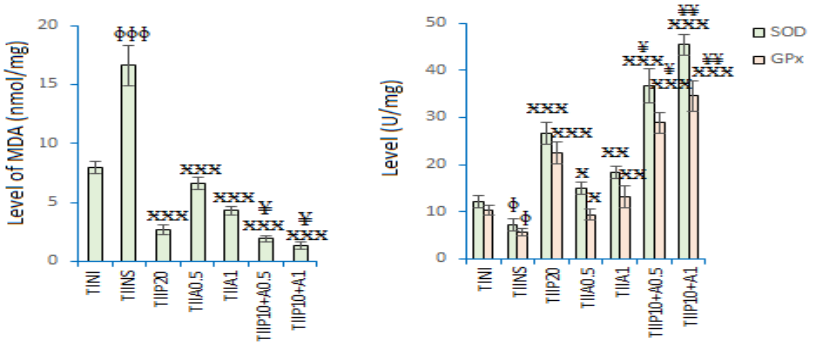

Fig. 2: Effects of AuNPs and PYR on tissue MDA levels and GPx and SOD enzyme activity in dexamethasone-immunosuppressed, *T. gondii*-infected mice. Data are expressed as mean ± SD (N=8). ϕ P<0.05, ϕϕϕ P<0.001 vs. TINI; ✕ P<0.05, ✕✕ P<0.01, ✕✕✕ P<0.001 vs. TIINS; ¥ P<0.05 vs. TIIP20

Evaluating the gene expression level by Real-time PCR

Real-time PCR analysis revealed that *T. gondii* infection in immunosuppressed mice significantly upregulated BAG1 and IL-4 expression while suppressing IFN-γ and IL-12 (P<0.001). Treatment-induced reversal of this profile was most pronounced in the TIIP10+A1 group (BAG1=1.08-fold, IL-4=1.09-fold, IFN-γ=4.92-fold, IL-12=5.24-fold; P=0.000) and TIIP10+A0.5 group (BAG1=1.22-fold, IL-4=1.19-fold, IFN-γ=4.21-fold, IL-12=4.23-fold; P=0.000), followed by TIIP20 (P=0.0015), TIIA1 (P=0.017), and TIIA0.5 (P=0.028), all relative to TIINS (P<0.001) (Fig. 3).

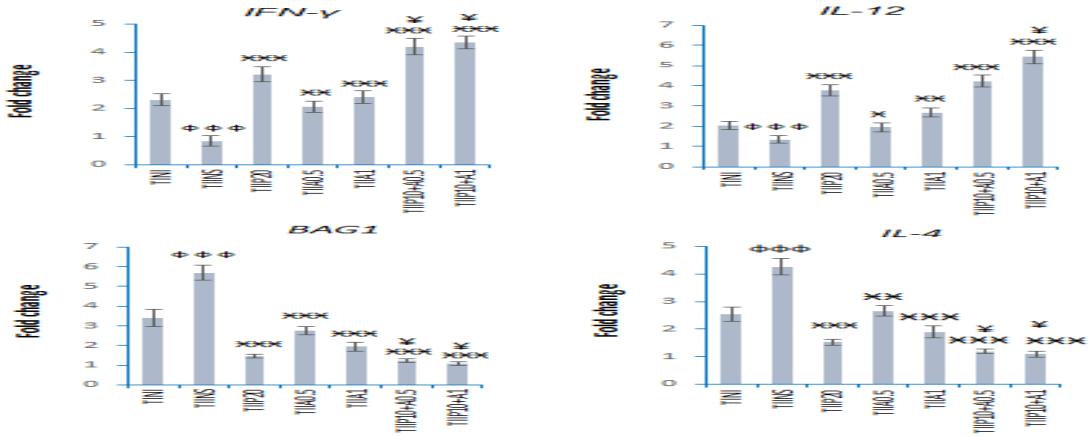

Fig. 3: Effects of AuNPs and PYR on expression levels of BAG1, IFN-γ, IL-12, and IL-4 in dexamethasone-immunosuppressed, *T. gondii*-infected mice. Data are expressed as mean ± SD (N=8). ϕϕϕ P<0.001 vs. TINI; ✕ P<0.05, ✕✕ P<0.01, ✕✕✕ P<0.001 vs. TIINS; ¥ P<0.05 vs. TIIP20

Biochemical and toxicological evaluation on vital organs

The biochemical assessments demonstrated a notable increase in serum concentrations of biomarkers associated with liver and kidney function in the mice of TINI and TIINS groups (P<0.001). ANOVA and *post hoc* analysis showed that after administration of AuNP, especially the combinations involving PYR (TIIP10+A0.5 and TIIP10+A1), there was a significant improvement (P<0.001) in the serum concentrations of AST, ALT, BUM, and Cr in the immunosuppressed mice infected with *T. gondii* (Fig. 4).

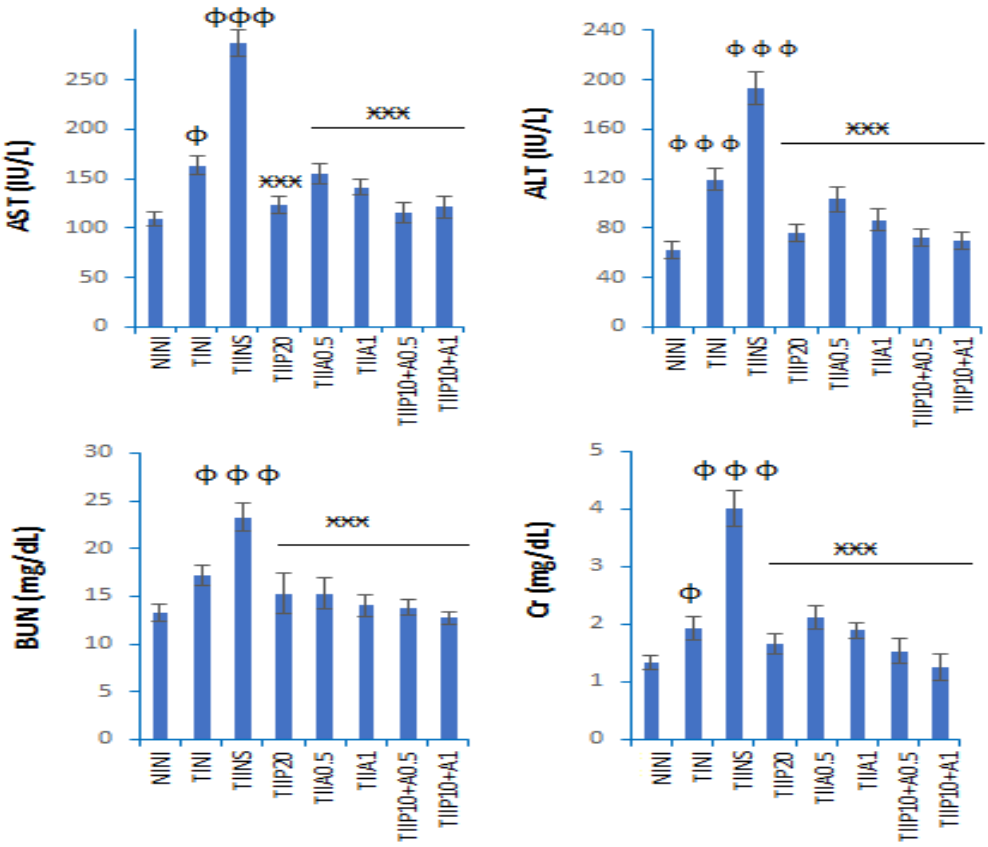

Fig. 4: Hepatorenal protective effects of AuNPs, alone and combined with PYR, on serum AST, ALT, BUN, and creatinine levels in dexamethasone-immunosuppressed, *T. gondii*-infected mice. Data are expressed as mean ± SD (N=8). ϕ P<0.05 vs. NINI; ϕϕϕ P<0.001 vs. TINI; ✖✖✖ P<0.001 vs. TIINS

Discussion

In this study, AuNPs green-synthesized using *S. khuzestanica* extract predominantly exhibited cubic morphology with an average size of 20–30 nm, consistent with previously reported AuNPs derived from plant extracts such as *Platycodon grandiflorum, Allium cepa,* and *Mentha spicata*, which ranged from 33–120 nm with spherical and cubic morphologies (11). Plant-derived phytochemicals—including polysaccharides, flavonoids, alkaloids, tannins, and saponins—serve as reducing and capping agents, facilitating Au^{3+} ion reduction and nanoparticle stabilization (11). FTIR analysis confirmed the involvement of multiple functional groups, with characteristic peaks at 1078, 1268, 3412, and 2936 cm^{-1} corresponding to C–O, C–O–C (oligosaccharides/triacylglycerols), O–H, and C–H stretch-

ing vibrations, respectively, alongside peaks at 1618–2029 cm^{-1} attributable to Csp^3–H, C=C, and C=O groups. These findings align with existing literature documenting Au^{3+} reduction mediated by flavonoids, tannins, proteins, and carboxylic acids (10, 11).

Treatment with AuNPs, particularly in the TIIP10+A0.5 and TIIP10+A1 groups, significantly improved survival rates and reduced both the number and size of *T. gondii* tissue cysts in immunosuppressed mice. These findings are consistent with reported antiparasitic activities of AuNPs across multiple parasitic infections: AuNPs demonstrated potent antileishmanial efficacy against *Leishmania donovani* promastigotes and amastigotes (IC_{50}: ~0.12 μg/mL) (21), inhibited *T. gondii* growth by over 90% (EC50 ≤7 μg/mL) (22), achieved >90% scolicidal elimination of *Echinococcus granulosus* protoscoleces at 0.3 mg/mL after 120 min (23), and exerted anthelmintic effects against *Raillietina* sp. at 1 mg/mL (24). Variability in efficacy across studies may reflect differences in synthesis methods and exposure duration. The antiparasitic mechanisms of AuNPs include inhibition of trypanothione reductase in *Leishmania*, blockade of falcipain-2 in *Plasmodium*, ROS generation, and interference with protein synthesis and DNA replication (10, 11).

BAG1, a cytoplasmic protein expressed at the onset of bradyzoite differentiation, serves as a definitive molecular marker for this stage and mediates specific T helper cell responses, while humoral immunity against bradyzoites predominates during early infection (25). The pathogenicity of *T. gondii* is fundamentally governed by its capacity to transition from the rapidly replicating, immunogenic tachyzoite stage to the dormant, less immunogenic bradyzoite stage encysted within host tissues—a shift that underpins parasite persistence and therapeutic resistance (26). Targeting the molecular regulators of this stage conversion therefore represents a compelling strategy for the development of cyst-eradicating chemotherapeutics (26). Notably, the present study demonstrated significant downregulation of BAG1 expression in treated mice, most prominently in the TIIP10+A0.5 and TIIP10+A1 groups, suggesting that AuNP–PYR combination therapy may impede bradyzoite differentiation and tissue cyst persistence.

The pathogenesis of *T. gondii* is linked to oxidative stress, which results in heightened release of free radicals and a reduced efficacy of the antioxidant enzymes (27). The interaction between pro-oxidant and antioxidant systems within the framework of toxoplasmosis and its treatment approaches has been addressed in prior academic discourse (27). Consequently, it is imperative to thoughtfully evaluate the integration of oxidant and/or antioxidant agents in the controlling of toxoplasmosis (27). We found that the administration of AuNP, particularly in the TIIP10+A0.5 and TIIP10+A1 groups, led to a significant reduction in MDA concentrations, as well as a marked increase in the levels of GPx and SOD. In their research, AuNP at the dose of 2.5 mg/kg enhance the activity of antioxidant enzymes, including glutathione (GSH), SOD, catalase, and GPx, in diabetic mice, effectively restoring their levels to those observed in non-diabetic subjects. This effect is attributed to the inhibition of lipid peroxidation and the generation of ROS during hyperglycemic conditions, thereby providing evidence of the antioxidant properties of AuNP in such metabolic states (28). The robust antioxidant properties of AuNP may play a significant role in the management of toxoplasmosis in immunocompromised mice.

Cell-mediated immunity is the cornerstone of host defense against *T. gondii*, with CD8+ and CD4+ T cells serving as primary effectors. Within the CD4+ compartment, Th1 cells drive IFN-γ, IL-2, and TNF-α production, with IFN-γ recognized as the critical cytokine mediating resistance across both acute infection and chronic toxoplasmic encephalitis (29). Th2-derived IL-4, by contrast, counter-

regulates Th1 polarization and promotes type-2 immune deviation—a dynamic that is exacerbated in dexamethasone-immunosuppressed hosts, where IFN-γ and IL-12 are markedly suppressed alongside transient IL-4 elevation (31). In the present study, AuNP treatment—most prominently in combination with PYR—reversed this immunological imbalance, significantly upregulating IFN-γ and IL-12 while suppressing IL-4 expression. This Th1-skewing effect is mechanistically supported by evidence that AuNPs promote dendritic cell maturation and augment IL-12 and IFN-γ secretion (32), collectively reinforcing cell-mediated effector responses. Taken together, restoration of Th1 polarization through AuNP–PYR-mediated immunomodulation likely constitutes a central mechanism underlying the observed therapeutic efficacy against *T. gondii* in the immunosuppressed murine model.

In relation to the protective effects of AuNP on essential organs, specifically the liver and kidneys, our biochemical evaluations indicated that following the administration of AuNP, particularly in conjunction with PYR in the combinations TIIP10+A0.5 and TIIP10+A1, there was a statistically significant enhancement (P<0.001) in the serum levels of AST, ALT, BUN, and Cr in immunosuppressed mice infected with *T. gondii*. Administration of AuNP at doses of 50 µg/kg, 100 µg/kg, and 150 µg/kg has been shown to mitigate acetaminophen-induced hepato-renal injury in rat models. This therapeutic effect is evidenced by the normalization of serum biomarkers, including ALT, AST, alkaline phosphatase, lactate dehydrogenase (LDH), cholesterol, bilirubin, albumin, urea, and creatinine, indicating protective effects on hepatic and renal function. However, a significant decrease in LPO and an elevation in GSH, SOD, and CAT levels were also noted in these subjects (33). The results of this investigation underscore the hepatoprotective and renoprotective properties of AuNP for controlling toxoplasmosis in immunocompromised mice.

Conclusion

AuNP, particularly in combination with PYR, demonstrates considerable efficacy against toxoplasmosis in immunosuppressed murine models. The underlying mechanisms likely encompass oxidative stress regulation, augmentation of antioxidant enzyme activity, and immunomodulation, with preservation of hepatic and renal function. Further pharmacodynamic and pharmacokinetic investigations—including assessments of bioavailability, absorption, and metabolic pathways—are warranted, alongside clinical trials to establish the safety profile and therapeutic potential of this combination approach.

Acknowledgements

This study was financially supported by Lorestan University of Medical Sciences, Khorramabad, Iran (Grant No. 1397-1-99-4515).

Conflict of interest

The authors declare that there is no conflict of interests.

Data availability

All supplementary data not published here will be sent to the respected readers for reasonable application. Please contact the corresponding author.

References

1. Innes EA. A brief history and overview of *Toxoplasma gondii*. Zoonoses Public Health. 2010;57(1):1-7.
2. Elsheikha HM, Marra CM, Zhu XQ. Epidemiology, pathophysiology, diagnosis, and management of cerebral toxoplasmosis. Clin Microbiol Rev. 2020;34(1): e00115-19.
3. Biesiada G, Kalinowska-Nowak A, Czepiel J, Mach T. Toxoplasmosis--epidemiology,

clinical manifestation and infection in pregnant women. Przegl Lek. 2006;63(2):97-9.
4. Teimouri A, Goudarzi F, Goudarzi K, Alimi R, Sahebi K, Foroozand H, Keshavarz H. *Toxoplasma gondii* Infection in Immunocompromised Patients in Iran (2013-2022): A Systematic Review and Meta-Analysis. Iran J Parasitol. 2022;17(4):443-457.
5. Dunay IR, Gajurel K, Dhakal R, Liesenfeld O, Montoya JG. Treatment of toxoplasmosis: historical perspective, animal models, and current clinical practice. Clin Microbiol Rev. 2018;31(4): e00057-17.
6. Cheraghipour K, Masoori L, Ezzatkhah F, et al. Effect of chitosan on *Toxoplasma gondii* infection: A systematic review. Parasite Epidemiol Contr. 2020;11:e00189.
7. Zhang Y, Bi J, Huang J, Tang Y, Du S, Li P. Exosome: A Review of Its Classification, Isolation Techniques, Storage, Diagnostic and Targeted Therapy Applications. Int J Nanomedicine. 2020;15:6917-6934.
8. Elahi N, Kamali M, Baghersad MH. Recent biomedical applications of gold nanoparticles: A review. Talanta. 2018;184:537-56.
9. Hammami I, Alabdallah NM. Gold nanoparticles: Synthesis properties and applications. J King Saud Univ Sci. 2021;33(7):101560.
10. Santhosh PB, Genova J, Chamati H. Green synthesis of gold nanoparticles: An eco-friendly approach. Chemistry. 2022;4(2):345-69.
11. Hashemi-Hafshejani S, Amani A, Azami SJ, et al. Nanoemulsion of spiramycin against tachyzoites of *Toxoplasma gondii*, RH strain: preparation, toxicology, and efficacy studies. Iran J Public Health. 2023;52(7):1495.
12. Goudarzi F, Jajarmi V, Shojaee S, Mohebali M, Keshavarz H. Formulation and evaluation of atovaquone-loaded macrophage-derived exosomes against *Toxoplasma gondii*: *in vitro* and *in vivo* assessment. Microbiol Spectr. 2024;12(1):e0308023.
13. Khaledi A, Meskini M. A Systematic Review of the Effects of *Satureja Khuzestanica* Jamzad and *Zataria Multiflora* Boiss against *Pseudomonas Aeruginosa*. Iran J Med Sci. 2020;45(2):83-90.
14. Sidorowicz A, Margarita V, Fais G, et al. Characterization of nanomaterials synthesized from Spirulina platensis extract and their potential antifungal activity. PLoS One. 2022;17(9):e0274753.
15. Maqbool Q, Yigit N, Stöger-Pollach M, et al. Operando monitoring of a room temperature nanocomposite methanol sensor. Catal Sci Technol. 2022;13(3):624-636.
16. Rehg JE, Hancock ML, Woodmansee DB. Characterization of a dexamethasonetreated rat model of cryptosporidial infection. J Infect Dis. 1988;158(6): 1406e1407.
17. Mahmoudvand H, Ziaali N, Ghazvini H, et al. *Toxoplasma gondii* infection promotes neuroinflammation through cytokine networks and induced hyperalgesia in BALB/c mice. Inflammation. 2016;39:405-12.
18. Baghdadi HB, Albalawi AE, Shater AF, Almohammed H, Alanazi AD. Linalool-zinc oxide nanocomposite controls *Toxoplasma gondii* infection through inhibiting inflammation, oxidative stress, and pathogenicity. J Basic Microbiol. 2024;64(8):e2400039.
19. Saadatmand M, Al-Awsi GR, Alanazi AD, et al. Green synthesis of zinc nanoparticles using *Lavandula angustifolia* Vera. Extract by microwave method and its prophylactic effects on *Toxoplasma gondii* infection. Saudi J Biol Sci. 2021;28(11):6454-60.
20. Mahmoudvand H, Kareshk AT, Moradi MN, et al. Efficacy and safety of *Zataria multiflora* Boiss essential oil against acute toxoplasmosis in mice. Iran J Parasitol. 2020;15(1):22-30.
21. Sasidharan S, Saudagar P. Gold and silver nanoparticles functionalized with 4', 7-dihydroxyflavone exhibit activity against *Leishmania donovani*. Acta Trop. 2022;231:106448.
22. Adeyemi OS, Murata Y, Sugi T, Kato K. Inorganic nanoparticles kill *Toxoplasma gondii* via changes in redox status and mitochondrial membrane potential. Int J Nanomedicine. 2017;12:1647-1661.

23. Barabadi H, Honary S, Ali Mohammadi M, et al. Green chemical synthesis of gold nanoparticles by using *Penicillium aculeatum* and their scolicidal activity against hydatid cyst protoscolices of *Echinococcus granulosus*. Environ Sci Pollut Res Int. 2017;24(6):5800-5810.
24. Kar PK, Murmu S, Saha S, Tandon V, Acharya K. Anthelmintic efficacy of gold nanoparticles derived from a phytopathogenic fungus, Nigrospora oryzae. PloS One. 2014;9(1):e84693.
25. Cerutti A, Blanchard N, Besteiro S. The bradyzoite: a key developmental stage for the persistence and pathogenesis of toxoplasmosis. Pathogens. 2020;9(3):234.
26. Selseleh M, Modarressi MH, Shojaee S, et al. Brain tissue cysts in infected mice with RH-strain of *Toxoplasma gondii* and evaluation of BAG1 and SAG1 genes expression. Iran J Parasitol. 2013;8(1):40-6.
27. Szewczyk-Golec K, Pawłowska M, Wesołowski R, Wróblewski M, Mila-Kierzenkowska C. Oxidative Stress as a Possible Target in the Treatment of Toxoplasmosis: Perspectives and Ambiguities. Int J Mol Sci. 2021; 22(11):5705.
28. Barathmanikanth S, Kalishwaralal K, Sriram M, et al. Anti-oxidant effect of gold nanoparticles restrains hyperglycemic conditions in diabetic mice. J Nanobiotechnology. 2010;8:16.
29. Jafari MM, Tabrizi ZA, Dayer MS, et al. Immune system roles in pathogenesis, prognosis, control, and treatment of *Toxoplasma gondii* infection. Int Immunopharmacol. 2023;124:110872.
30. Khan IA, Moretto M. Immune responses to *Toxoplasma gondii*. Curr Opin Immunol. 2022;77:102226.
31. Kang KN, Choi IU, Shin DW, Lee YH. Cytokine and antibody responses of reactivated murine toxoplasmosis upon administration of dexamathasone. Korean J Parasitol. 2006;44(3):209-19.
32. Huang H, Liu R, Yang J, et al. Gold Nanoparticles: Construction for Drug Delivery and Application in Cancer Immunotherapy. Pharmaceutics. 2023;15(7):1868.
33. Reshi MS, Shrivastava S, Jaswal A, Sinha N, Uthra C, Shukla S. Gold nanoparticles ameliorate acetaminophen induced hepato-renal injury in rats. Exp Toxicol Pathol. 2017;69(4):231-240.